

Full Length Research Paper

Quinazolin derivatives as eco-friendly corrosion inhibitors for low carbon steel in 2 M HCl solutions

A. S. Fouda*, G. Y. Elewady, H. A. Mostafa and S. Habbouba

Department of Chemistry, Faculty of Science, El -Mansoura University, El-Mansoura-35516, Egypt.

Accepted 13 May 2013

Some quinazoline derivatives such as: 3-(4-chlorophenyl)-2-methylquinazolin-4(3H)-one (CMQ) and 2-methyl-3-(4-nitrophenyl) quinazolin-4(3H)-one (MNQ) were investigated as corrosion inhibitors for carbon steel in 2 M HCl solution. Electrochemical impedance spectroscopy (EIS), potentiodynamic polarization, electrochemical frequency modulation and weight loss methods were used to study the inhibition action at 30°C. The corrosion of steel was controlled by a charge transfer process at the prevailing conditions. The electrochemical results showed that these compounds are efficient inhibitors for carbon steel and efficiency up to 93.8% was obtained at 30°C. The inhibition efficiency increases with inhibitor concentration. The adsorption of these compounds on carbon steel surface follows the Langmuir adsorption isotherm. Polarization curves indicate that investigated quinazoline derivatives are mixed-type inhibitors. The chemical and electrochemical methods gave similar results.

Key words: Corrosion inhibitors, hydrogen acid (HCl), carbon steel, quinazoline derivatives.

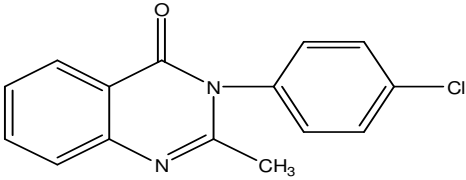
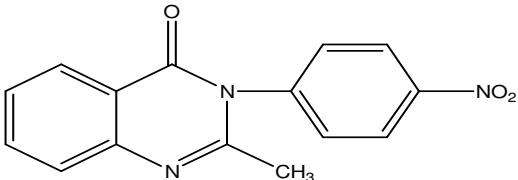
INTRODUCTION

Carbon steel has been extensively used under different conditions in petroleum industries (Deyab, 2007). Aqueous solutions of acids are among the most corrosive media and are widely used in industries for pickling, acid cleaning of boilers, descaling and oil well (Abd El-Maksous et al., 2005; Machnikova et al., 2008 a,b; Khaled, 2008; Ashassi-sorkhabi et al., 2004; Migahed and Nasser 2008). The main problem concerning carbon steel applications its relatively low corrosion resistance in acidic solution. Several methods used currently to prevent corrosion of carbon steel. One of such methods is the use of organic inhibitors (Avci, 2008; Pillali and Narayan 1985; O'M Bockris and Yang 1991; Jovancevic et al., 1988; Uhera and Aramaki, 1991; Akust et al., 1982; Abdallah et al., 2006; Ishtiaque et al., 2010; Fouda et al., 2006 a,b). Effective inhibitors are heterocyclic compounds that have π bonds, heteroatoms such as

sulphur, oxygen and nitrogen (Benali et al., 2007). Compounds containing both nitrogen and chloro atoms can provide excellent inhibition, compared with compounds containing only nitrogen- or chloro- atom (Abboud et al., 2007). Heterocyclic compounds such as quinazolin can provide excellent inhibition. These molecules depend mainly on certain physical properties of the inhibitor molecules such as functional groups, steric factors, electron density at the donor atom and electronic structure of the molecules (Khaled, 2003; Popova et al., 2004). Regarding the adsorption of the inhibitor on the metal surface, two types of interactions are responsible. One is physical adsorption which involves electrostatic force between ionic charges or dipoles of the adsorbed species and electric charge at metal/ solution interface. Others are chemical adsorption, which involves charge sharing or charge transfer from

*Corresponding author. E-mail: asfouda@mans.edu.eg. Tel: +02 050 2365730. Fax:+02 050 2446254.

Table 1. Molecular structure, formula and molecular weight of investigated compounds.

| Inhibitor | Structure formula | Molecular formula and weight |
|--|--|--|
| CMQ 3-(4-chlorophenyl)-2-methylquinazolin-4(3H)-one |  | C ₁₅ H ₁₁ ClN ₂ O 270.056 |
| MNQ 2-methyl-3-(4-nitrophenyl)quinazolin-4(3H)-one |  | C ₁₅ H ₁₁ N ₃ O ₃ 281.080 |

inhibitor molecules to the metal surface to form coordinated types of bonds (Noot and Moubaraki 2008). The selection of appropriate inhibitors mainly depends on the type of acid, its concentration, and temperature. In the present work, the inhibition characteristics of 3-(4-chlorophenyl)-2-methylquinazolin-4(3H)-one and 2-methyl-3-(4-nitrophenyl)quinazolin-4(3H)-one for carbon steel in HCl solution were investigated using chemical and electrochemical techniques.

EXPERIMENTAL

Chemicals and materials

Hydrochloric acid (37%), ethyl alcohol and acetone were purchased from Al-Gamhoria Company, Egypt, 3-(4-Chlorophenyl)-2-methylquinazolin-4(3H)-one (CMQ) and 2-Methyl-3-(4-nitrophenyl)quinazolin-4(3H)-one (MNQ) were synthesized as described before (Gao et al., 2007) and the purity of the compounds was checked by thin layer chromatography (TLC). The molecular structures and other details of these compounds are given in Table 1. Bidistilled water was used throughout all the experiments. The chemical composition of low carbon steel (weight %) was: C= 0.14-0.20, Mn= 0.6-0.9, P= 0.04, S= 0.05 and the rest is iron.

Methods

Weight loss measurements

Rectangular specimens of carbon steel with dimensions 2.1 × 2.0 × 0.2 cm were mechanically abrading with different grades of emery paper, degreased with acetone, rinsed with bidistilled water and dried between filter papers. After weighting accurately, the specimens were immersed in 100 ml of 2 M HCl with and without different concentrations of inhibitors at 30°C. After different immersion periods (each of 30 min till 180 min), carbon steel samples were taken out, washed with bidistilled water, dried and weighted again. The weight loss values are used to calculate the corrosion rate (R) in mmy⁻¹ by the relation:

$$R = (\text{weight loss in gram} \times 8.75 \times 10^4) / \text{DAT} \quad (1)$$

where D is carbon steel density in g cm⁻³, A is exposed area in cm², T is exposure time in hour. The inhibition efficiency (%Y_w) and the degree of surface coverage (θ) were calculated from Equation (2):

$$\%Y_w = \theta \times 100 = [(R^* - R) / R^*] \times 100 \quad (2)$$

where R^{*} and R are the corrosion rates of carbon steel in the absence and in the presence of inhibitor, respectively.

Electrochemical measurements

Electrochemical measurements were conducted in a conventional three electrodes cell assembly. A platinum foil and saturated calomel electrode (SCE) were used as counter and reference electrodes, respectively. The carbon steel electrodes were 1 × 1 cm and were welded from one side to a copper wire used for electrical connection. The electrodes were abraded, degreased and rinsed as described in weight loss measurements. All experiments were carried out at temperature (30 ± 1°C). The potentiodynamic curves were recorded from -500 to 500 mV at a scan rate 1 mV S⁻¹ after the steady state is reached (30 min) and the open circuit potential (OCP) was noted. The Y_p% and degree of surface coverage were calculated from Equation (3):

$$Y_p\% = \theta \times 100 = [1 - (i_{\text{corr}}^{\circ} / i_{\text{corr}})] \times 100 \quad (3)$$

where i_{corr}^o and i_{corr} are the corrosion current densities of uninhibited and inhibited solution, respectively.

Electrochemical impedance spectroscopy (EIS) and electrochemical frequency modulation (EFM) experiments were carried out using Gamry Potentiostat/Galvanostat/ZRA (model PCI4/300) with a Gamry framework system based on ESA400. Gamry applications include software EIS300 for EIS measurements and EFM140 for EFM measurements, computer was used for collecting data. Echem Analyst 5.5 Software was used for plotting, graphing and fitting data. EIS measurements were carried out in a frequency range of 100 kHz to 100 mHz with amplitude of 5 mV peak-to-peak using ac signals at respective corrosion potential. EFM carried out using two frequencies 2 and 5 Hz. The base

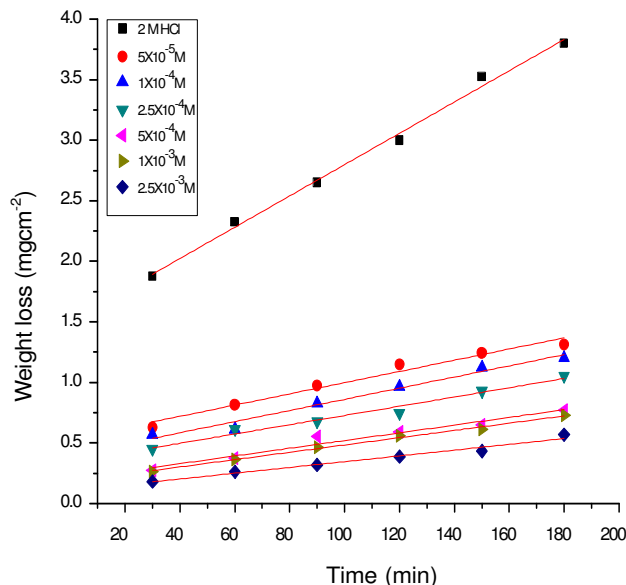


Figure 1. Weight loss-time curves of carbon steel in 2 M HCl in the absence and presence of different concentrations of CMQ at 30°C.

Table 2. Data of weight loss measurements for carbon steel in 2 M HCl solution in the absence and presence of different concentrations of investigated compounds at 30°C.

| Compound | Conc. (M) | R (mg cm ⁻² min ⁻¹) | θ | Y _w (%) |
|----------|----------------------|--|----------|--------------------|
| Blank | 0.00 | 0.0250 | 0.000 | 00.0 |
| | 5.0×10 ⁻⁵ | 0.0096 | 0.610 | 61.0 |
| | 1×10 ⁻⁴ | 0.0083 | 0.678 | 67.8 |
| | 2.5×10 ⁻⁴ | 0.0062 | 0.750 | 75.0 |
| | 5.0×10 ⁻⁴ | 0.0049 | 0.800 | 80.0 |
| | 1×10 ⁻³ | 0.0041 | 0.814 | 81.4 |
| | 2.5×10 ⁻³ | 0.0032 | 0.872 | 87.2 |
| MNQ | 5.0×10 ⁻⁵ | 0.0170 | 0.330 | 33.0 |
| | 1×10 ⁻⁴ | 0.0150 | 0.407 | 40.7 |
| | 2.5×10 ⁻⁴ | 0.0082 | 0.477 | 47.7 |
| | 5.0×10 ⁻⁴ | 0.0068 | 0.720 | 72.0 |
| | 1×10 ⁻³ | 0.0057 | 0.761 | 76.1 |
| | 2.5×10 ⁻³ | 0.0056 | 0.772 | 77.2 |

frequency was 1 Hz. In this study, we use a perturbation signal with amplitude of 10 mV for both perturbation frequencies of 2 and 5 Hz.

RESULTS AND DISCUSSION

Weight loss measurements

Figure 1 shows the weight loss-time curves for the

corrosion of carbon steel in 2 M HCl in the absence and presence of different concentrations of CMQ. Similar curves for MNQ were obtained (not shown). The data of Table 2 show that, the inhibition efficiency increases with increase in inhibitor concentration from 0.05 to 2.5 mmol l⁻¹.

The maximum inhibition efficiency was achieved at 2.5 mmol l⁻¹. The lowest corrosion rate is obtained in the presence of MNQ, therefore Y_w% tends to decrease in the following order: CMQ > MNQ.

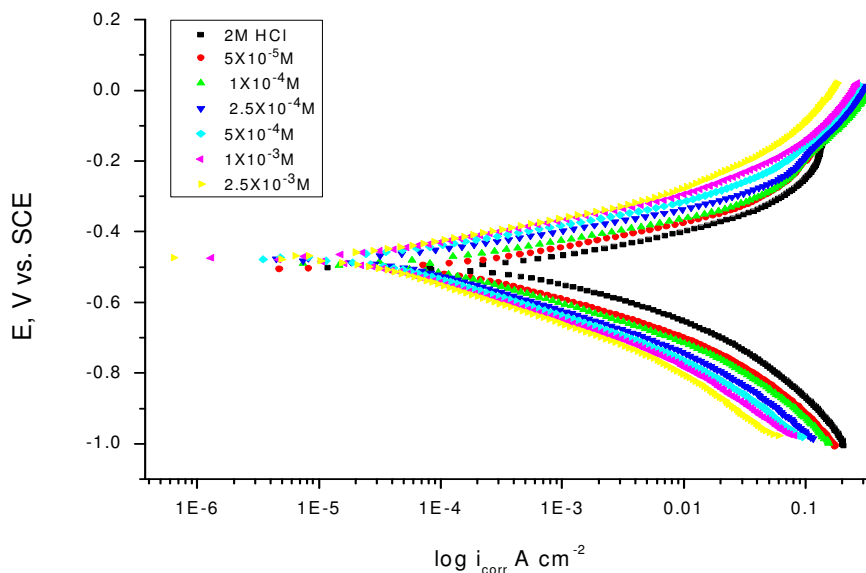


Figure 2. Potentiodynamic polarization for corrosion of carbon steel in 2 M HCl in the absence and presence of different concentrations of CMQ at 30°C.

Electrochemical measurements

Potentiodynamic polarization measurements

The potentiodynamic curves for carbon steel in 2 M HCl in the absence and presence of CMQ are shown in Figure 2. Similar curves were obtained for MNQ (not shown). It is clear that; the investigated inhibitors affect the promoting retardation of anodic dissolution of carbon steel and cathodic hydrogen discharge reactions. Electrochemical parameters such as corrosion current density (i_{corr}), corrosion potential (E_{corr}), Tafel constants (β_a and β_c), degree of surface coverage (θ) and inhibition efficiency ($\%Y_p$) were calculated from Tafel plots and are given in Table 3. It is observed that the presence of inhibitor lowers i_{corr} . Maximum decrease in i_{corr} values was observed for CMQ indicating that this is the most effective corrosion inhibitor. It is also observed from Table 3 that E_{corr} values and Tafel slope constants do not change significantly in inhibited solution as compared to uninhibited solution. The investigated compounds do not shift the E_{corr} values significantly, suggesting that they behave as mixed type inhibitors (Ajmal et al., 1994). Both cathodic (β_c) and anodic (β_a) Tafel lines are parallel. This indicates that the mechanism of the corrosion reaction does not change and the corrosion reaction is inhibited by simple adsorption mode (Bentiss et al., 2005). Also, cathodic and anodic Tafel lines were shifted to more negative and positive direction, respectively by adding inhibitors. This suggesting that these inhibitors behave as mixed type inhibitors. The irregular trends of β_a and β_c values indicate the involvement of more than

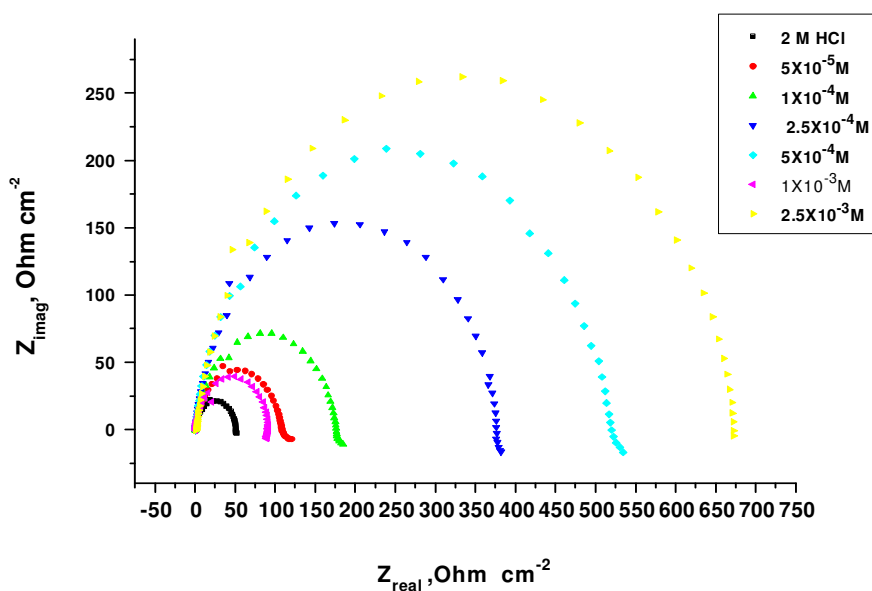
one type of species adsorbed on the metal surface. The order of inhibition efficiency is as follows (Table 3): CMQ > MNQ.

Electrochemical impedance spectroscopy

The EIS provides important mechanistic and kinetic information for an electrochemical system under investigation. Nyquist impedance plots obtained for the steel electrode at respective corrosion potentials after 30 min immersion in 2 M HCl in the presence and absence of various concentrations of CMQ is shown in Figure 3 (MNQ curves not shown). This diagram exhibits a single semi-circle shifted along the real impedance (Z_r). The Nyquist plots of CMQ do not yield perfect semicircles as expected from the theory of EIS, the impedance loops measured are depressed semi-circles with their centers below the real axis, where the kind of phenomenon is known as the “dispersing effect” as a result of frequency dispersion (Achouri et al., 2001) and mass transport resistant (Khaled, 2003) as well as electrode surface heterogeneity resulting from surface roughness, impurities, dislocations, grain boundaries, adsorption of inhibitors, formation of porous layers (Growcock and Jasinski, 1989; Rammet and Reinhart 1987; Mehaute and Grep 1983; Machnikova et al., 2008 a,b; Hsu and Mansfeld 2001; Lebrini et al., 2007), etc so one constant phase element (CPE) is substituted for the capacitive element, to explain the depression of the capacitance semi-circle, to give a more accurate fit. Impedance data are analyzed using the circuit in Figure 4; in which R_s

Table 3. Potentiodynamic data of carbon steel in 2 M HCl and in the presence of different concentrations of inhibitors at 30°C.

| Compound | Conc. (M) | $-E_{\text{corr}}$, mVvs.SCE | i_{corr} $\mu\text{A cm}^{-2}$ | $-\beta_c$, mVdec $^{-1}$ | β_a , mVdec $^{-1}$ | θ | Y_p (%) | R , mmy $^{-1}$ |
|----------|----------------------|-------------------------------|---|----------------------------|---------------------------|----------|-----------|-------------------|
| CMQ | Blank | 499 | 359.0 | 98 | 69 | 0.000 | 00.0 | 164.1 |
| | 5×10^{-5} | 504 | 139.0 | 101 | 69 | 0.618 | 61.8 | 71.0 |
| | 1×10^{-4} | 492 | 76.6 | 102 | 60 | 0.787 | 78.7 | 38.9 |
| | 2.5×10^{-4} | 479 | 41.1 | 107 | 59 | 0.886 | 88.6 | 20.8 |
| | 5×10^{-4} | 476 | 29.8 | 108 | 62 | 0.917 | 91.7 | 15.3 |
| | 1×10^{-3} | 476 | 23.7 | 110 | 67 | 0.930 | 93.0 | 12.2 |
| | 2.5×10^{-3} | 474 | 21.1 | 116 | 71 | 0.938 | 93.8 | 11.0 |
| MNQ | 5×10^{-5} | 494 | 141.0 | 103 | 71 | 0.590 | 59.0 | 71.2 |
| | 1×10^{-4} | 503 | 127.0 | 93 | 55 | 0.610 | 61.0 | 75.2 |
| | 2.5×10^{-4} | 499 | 120.0 | 101 | 60 | 0.665 | 66.5 | 63.5 |
| | 5×10^{-4} | 490 | 73.6 | 108 | 61 | 0.795 | 79.5 | 37.7 |
| | 1×10^{-3} | 487 | 46.6 | 109 | 65 | 0.870 | 87.0 | 24.8 |
| | 2.5×10^{-3} | 471 | 31.2 | 117 | 69 | 0.913 | 91.3 | 16.9 |

**Figure 3.** Nyquist plots for carbon steel in 2 M HCl at different concentrations of CMQ.

represents the electrolyte resistance, R_{ct} represents the charge-transfer resistance and the constant phase element (CPE). According to Hsu and Mansfeld (2001) the correction of capacity to its real values is calculated from:

$$C_{\text{dl}} = Y_o (\omega_{\text{max}})^{n-1} \quad (4)$$

where Y_o is the CPE coefficient, ω_{max} is the frequency at which the imaginary part of impedance ($-Z_i$) has a maximum and n is the CPE exponent (phase shift).

The data obtained from fitted spectra are listed in Table 4. The degree of surface coverage (θ) and the inhibition efficiency ($Y_1\%$) were calculated from Equation (5):

$$Y_1 \% = \theta \times 100 = [1 - (R_{\text{ct}} / R_{\text{ct}}^*)] \times 100 \quad (5)$$

where R_{ct} and R_{ct}^* are the charge-transfer resistances with and without the inhibitors, respectively.

Data in Table 4 show that; the R_s values are very small compared to the R_{ct} values. Also; the R_{ct} values increase and the calculated C_{dl} values decrease by increasing the

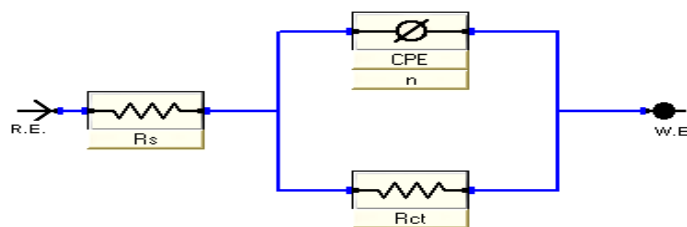


Figure 4. Equivalent circuit model used to fit the impedance spectra.

Table 4. EIS data of carbon steel in 2 M HCl and in the presence of different concentrations of inhibitors at 30°C.

| Comp. | Conc. (M) | $R_s \Omega \text{ cm}^2$ | $Y \mu\Omega^{-1} \text{ s}^n \text{ cm}^{-2}$ | n | $R_{CT} \Omega \text{ cm}^2$ | $C_{dl} \mu\text{F cm}^{-2}$ | θ | Y_i (%) | |
|----------------------|----------------------|---------------------------|--|-------|------------------------------|------------------------------|----------|-----------|------|
| Blank | 0.0 | 0.855 | 135.9 | 0.923 | 50.2 | 177.3 | 0.00 | 0.00 | |
| | 5.0×10^{-5} | 0.769 | 67.3 | 0.930 | 107.0 | 85.1 | 0.530 | 53.0 | |
| | 1×10^{-4} | 0.724 | 49.3 | 0.941 | 171.0 | 72.8 | 0.707 | 70.7 | |
| | CMQ | 2.5×10^{-4} | 0.788 | 37.8 | 0.929 | 367.0 | 47.3 | 0.863 | 86.3 |
| | | 5.0×10^{-4} | 0.903 | 36.2 | 0.919 | 502.9 | 45.7 | 0.900 | 90.0 |
| | | 1×10^{-3} | 1.33 | 43.5 | 0.907 | 654.5 | 42.3 | 0.923 | 92.3 |
| 2.5×10^{-3} | 0.952 | 42.2 | 0.890 | 700.6 | 40.1 | 0.928 | 92.8 | | |
| MNQ | 5.0×10^{-5} | 0.995 | 34.7 | 1.020 | 89.95 | 85.9 | 0.440 | 44.0 | |
| | 1×10^{-4} | 0.887 | 55.6 | 0.924 | 122.9 | 72.1 | 0.590 | 59.0 | |
| | 2.5×10^{-4} | 0.842 | 50.6 | 0.936 | 155.8 | 70.0 | 0.670 | 67.0 | |
| | 5.0×10^{-4} | 0.903 | 48.11 | 0.921 | 202.1 | 61.3 | 0.750 | 75.0 | |
| | 1×10^{-3} | 0.941 | 43.1 | 0.920 | 330.1 | 54.2 | 0.850 | 85.0 | |
| | 2.5×10^{-3} | 1.06 | 37.5 | 0.906 | 415.0 | 48.6 | 0.880 | 88.0 | |

inhibitor concentrations, which causes an increase of θ and Y_i . The high R_{ct} values are generally associated with slower corroding system (Bosch et al., 2001). The decrease in the C_{dl} suggests that inhibitors function by adsorption at the metal/solution interface.

The inhibition efficiency, calculated from EIS results, show the same trend as those obtained from polarization measurements. The difference of inhibition efficiency from two methods may be attributed to the different surface status of the electrode in two measurements. EIS were performed at the rest potential, while in polarization measurements the electrode potential was polarized to high over potential, non-uniform current distributions, resulted from cell geometry, solution conductivity, counter and reference electrode placement, etc., will lead to the difference between the electrode area actually undergoing polarization and the total area (Kelly et al., 2002).

Electrochemical frequency modulation (EFM)

EFM is a nondestructive corrosion measurement like EIS; it is a small signal technique. Unlike EIS, however, two sine waves (at different frequencies) are applied to the cell simultaneously. The great strength of the EFM is the

causality factors which serve as an internal check on the validity of the EFM measurement (Donahue and Nobe, 1965). With the causality factors the experimental EFM data can be verified.

The results of EFM experiments are a spectrum of current response as a function of frequency. The spectrum is called the intermodulation spectrum. The spectra contain current responses assigned for harmonical and intermodulation current peaks. The larger peaks were used to calculate the corrosion current density (i_{corr}), the Tafel slopes (β_c and β_a) and the causality factors (CF-2 and CF-3). Intermodulation spectra obtained from EFM measurements are presented in Figure 5 for 2 M HCl in absence and presence of 2.5×10^{-3} M of CMQ and MNQ respectively. Similar curves were obtained for other inhibitors (not shown). Table 6 indicated that; the corrosion current densities decrease by increasing the concentrations of the studied inhibitors. The inhibition efficiencies, $Y_{EFM}\%$ calculated from Equation 6 increase with increasing the studied inhibitor concentrations:

$$Y_{EFM} \% = \frac{i_{corr}^0 - i_{corr}}{i_{corr}^0} \times 100 \quad (6)$$

where: i_{corr}^0 and i_{corr} are corrosion current densities in the

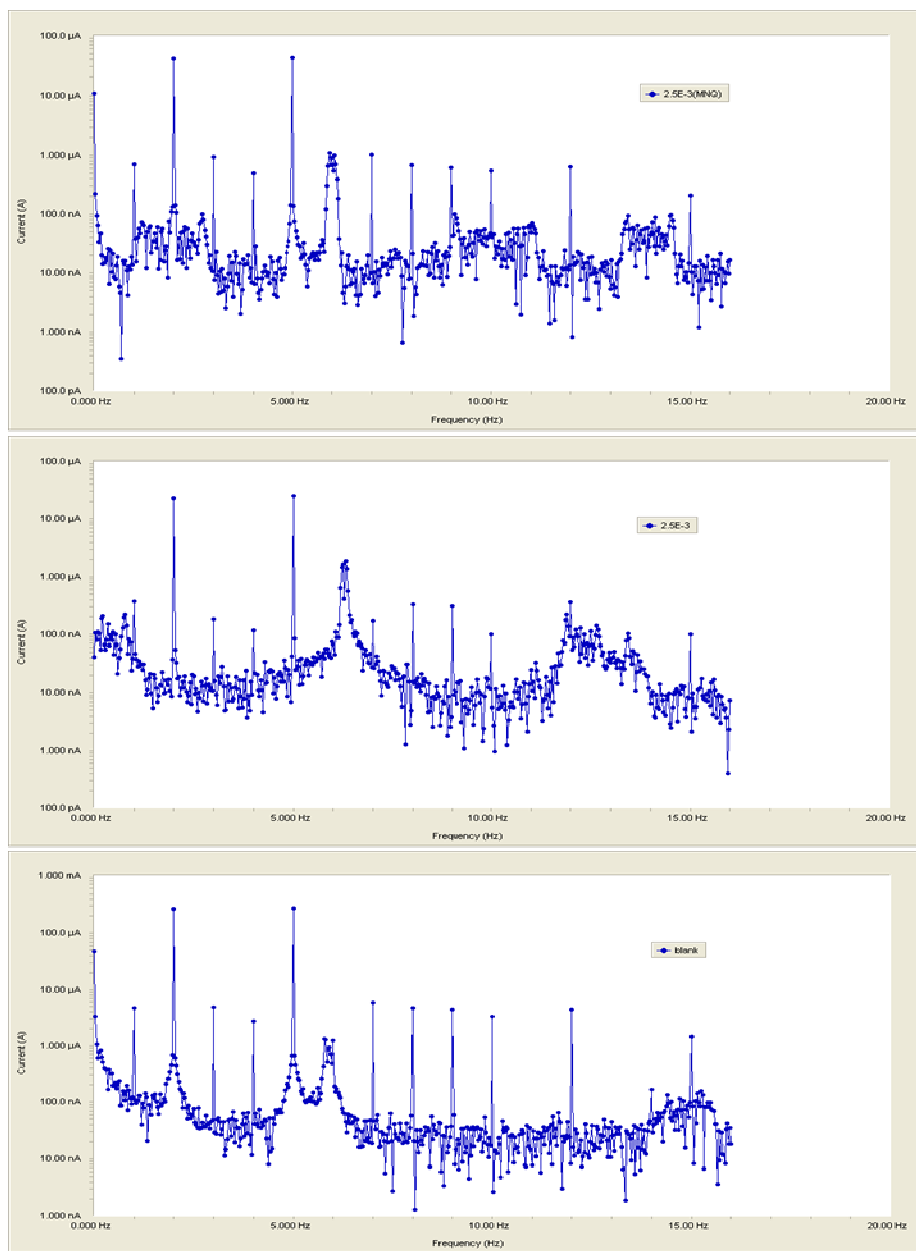


Figure 5. Intermodulation spectra for carbon steel in 2 M HCl in the absence and presence of 2.5×10^{-3} M CMQ and NMQ.

absence and presence of inhibitors, respectively. The causality factors in Table 5 are very close to theoretical values which according to the EFM theory (Khamis et al., 1991) should guarantee the validity of Tafel slopes and corrosion current densities.

Adsorption isotherm

The mode and extent of the interaction between inhibitor and the iron surface can be studied by applying

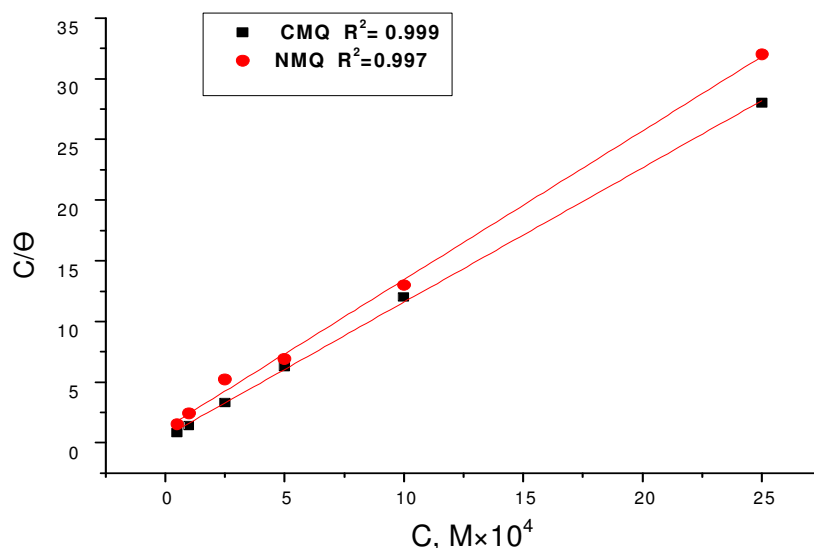
adsorption isotherms. The degree of surface coverage, θ , at different inhibitor concentrations in 2 M HCl was evaluated from weight loss measurements ($\theta = IE/100$) and is given in Table 2. The fitting to the Langmuir isotherm is shown by plotting C/θ versus C (Figure 6) according to the following equation (Zhao and Mu 1999):

$$C/\theta = 1/K_{\text{ads}} + C \quad (7)$$

$$K_{\text{ads}} C = 1/55.5 \exp(-\Delta G_{\text{ads}}^{\circ}) \quad (8)$$

Table 5. Electrochemical kinetic parameters obtained by EFM technique for carbon steel the absence and in presence of various concentrations of inhibitors in 2 M HCl at 30°C.

| Compound | Conc. (M) | $j_{\text{corr}} \mu\text{A cm}^{-2}$ | $\beta_c \text{ mVdec}^{-1}$ | $\beta_a \text{ mVdec}^{-1}$ | CF-2 | CF-3 | C.R mmy^{-1} | $Y_{\text{EFM}} (\%)$ |
|----------------------|----------------------|---------------------------------------|------------------------------|------------------------------|------|------|-----------------------|-----------------------|
| Blank | 0.00 | 373.5 | 95.1 | 85.2 | 1.78 | 3.33 | 166.6 | 0.00 |
| | 5×10^{-5} | 161.7 | 101.1 | 81.9 | 1.95 | 3.29 | 80.1 | 56.7 |
| | 1×10^{-4} | 108.3 | 101.5 | 83.9 | 1.89 | 2.06 | 53.7 | 71.0 |
| | 2.5×10^{-4} | 55.3 | 99.9 | 88.5 | 2.09 | 2.88 | 27.4 | 85.1 |
| | 5.0×10^{-4} | 42.3 | 102.3 | 91.9 | 2.01 | 1.79 | 20.9 | 88.6 |
| | 1×10^{-3} | 35.4 | 99.9 | 92.1 | 1.59 | 3.60 | 17.6 | 90.5 |
| | 2.5×10^{-3} | 32.4 | 98.3 | 94.1 | 2.11 | 3.04 | 16.3 | 91.2 |
| CMQ | 5×10^{-5} | 210.6 | 93.6 | 83.9 | 2.29 | 4.6 | 106.9 | 43.6 |
| | 1×10^{-4} | 190.1 | 101.2 | 81.3 | 1.94 | 2.86 | 94.2 | 49.1 |
| | 2.5×10^{-4} | 153.1 | 99.9 | 84.4 | 1.91 | 1.42 | 76.1 | 58.1 |
| | 5.0×10^{-4} | 94.3 | 98.3 | 86.3 | 1.94 | 1.83 | 46.9 | 74.6 |
| | 1×10^{-3} | 86.9 | 99.1 | 86.9 | 1.87 | 1.19 | 29.6 | 83.9 |
| | 2.5×10^{-3} | 49.6 | 96.2 | 90.9 | 1.80 | 1.91 | 26.3 | 86.7 |
| | MNQ | 5×10^{-5} | 210.6 | 93.6 | 83.9 | 2.29 | 4.6 | 106.9 |
| 1×10^{-4} | | 190.1 | 101.2 | 81.3 | 1.94 | 2.86 | 94.2 | 49.1 |
| 2.5×10^{-4} | | 153.1 | 99.9 | 84.4 | 1.91 | 1.42 | 76.1 | 58.1 |
| 5.0×10^{-4} | | 94.3 | 98.3 | 86.3 | 1.94 | 1.83 | 46.9 | 74.6 |
| 1×10^{-3} | | 86.9 | 99.1 | 86.9 | 1.87 | 1.19 | 29.6 | 83.9 |
| 2.5×10^{-3} | | 49.6 | 96.2 | 90.9 | 1.80 | 1.91 | 26.3 | 86.7 |

**Figure 6.** Langmuir adsorption plots for carbon steel in 2 M HCl containing various concentration of inhibitors.

where C is the inhibitor concentration, θ is the fraction of the surface coverage, K_{ads} is the modified adsorption equilibrium constant which can be related to the free energy of adsorption $\Delta G_{\text{ads}}^{\circ}$ and 55.5 is the molar concentration of water in mol L^{-1} . In this case, linear plots with high correlation coefficients and slopes of about unity were obtained, indicating that the experimental results fit the Langmuir isotherm. The values of the correlation coefficients, free energy of adsorption ($\Delta G_{\text{ads}}^{\circ}$) and the adsorption equilibrium constants are given in Table 6. The regression coefficient (R^2) is more than 0.99 suggests a good relation between C/θ and C . The values

of $\Delta G_{\text{ads}}^{\circ}$ recorded in Table 6 are negative, suggesting the spontaneity of the adsorption process. It is well known that values of $\Delta G_{\text{ads}}^{\circ}$ in the order of 20 kJ mol^{-1} or lower indicate a physisorption, while those of order of 40 kJ mol^{-1} or higher involve charge sharing or charge transfer from the inhibitor molecules to the metal surface to form a coordinate type of bond (chemisorption) (Donahue and Nobe, 1965). The calculated $\Delta G_{\text{ads}}^{\circ}$ values for CMQ and MNQ in 2 M HCl are 35.2 kJ mol^{-1} and 32.4 kJ mol^{-1} , respectively. This indicates that an electrostatic interaction exists (physisorption) between inhibitor and the charged metal surface. The K_{ads} value for CMQ is

Table 6. Values of adsorption isotherm parameters.

| Inhibitor | Temp. K | Adsorption isotherm | $K_{ads} M^{-1}$ | slope | $-\Delta G^{\circ}_{ads}, kJ mol^{-1}$ | R^2 |
|-----------|---------|---------------------|------------------|-------|--|--------|
| CMQ | 303 | Langmuir | 2.4 | 1.02 | 35.2 | 0.9994 |
| MNQ | | | 2.1 | 1.0 | 32.4 | 0.9998 |

larger than its value for compound MNQ, so compound CMQ strongly adsorbed on carbon steel surface than compound MNQ. The lower K_{ads} values indicate that these compounds are adsorbed physically on carbon steel surface.

Mechanism of corrosion inhibition

The adsorption of quionazolin derivatives can be attributed to the presence of polar unit having atoms of nitrogen and oxygen and aromatic/heterocyclic rings. Therefore, the possible reaction centers are unshared electron pair of hetero-atoms and π -electrons of aromatic ring (Ahamad et al., 2010). The adsorption and inhibition effect of quionazolin derivatives in 2 M HCl solution can be explained as follows: In aqueous acidic solutions, quionazolin derivatives exist either as neutral molecules or as protonated molecules and may adsorb on the metal/acid solution interface by one and/or more of the following ways: (i) electrostatic interaction of protonated molecules with already adsorbed chloride ions, (ii) donor-acceptor interactions between the π -electrons of aromatic ring and vacant d orbital of surface iron atoms, (iii) interaction between unshared electron pairs of hetero-atoms and vacant d-orbital of iron surface atoms. In general, two modes of adsorption are considered on the metal surface in acid media. In the first mode, the neutral molecules may be adsorbed on the surface of carbon steel through the chemisorption mechanism, involving the displacement of water molecules from the carbon steel surface and the sharing electrons between the hetero-atoms and iron. The inhibitor molecules can also adsorb on the carbon steel surface on the basis of donor-acceptor interactions between π -electrons of the aromatic ring and vacant d-orbitals of surface iron atoms. In the second mode, since it is well known that the steel surface bears positive charge in acid solution (Singh and Quraishi 2010), so it is difficult for the protonated molecules to approach the positively charged carbon steel surface due to the electrostatic repulsion. Since chloride ions have a smaller degree of hydration, thus they could bring excess negative charges in the vicinity of the interface and favor more adsorption of the positively charged inhibitor molecules, the protonated quionazolin derivatives adsorb through electrostatic interactions between the positively charged molecules and the negatively charged metal surface. Thus there is a synergism between adsorbed Cl^- ions and protonated

quionazolin derivatives. Thus we can conclude that inhibition of carbon steel corrosion in 2 M HCl is mainly due to electrostatic interaction. The decrease in inhibition efficiency with rise in temperature supports electrostatic interaction.

Variation in structure of inhibitors molecules takes place through the phenyl group. Hence, the inhibition efficiency depends on this part of the molecule. The order of decreasing inhibition efficiency of these compounds is as follows: $-Cl > -NO_2$. This order of decreased inhibition efficiency was interpreted by the terms of polar effect (Hammett, 1940) of the p-substitute's on phenyl group. Investigated quionazolin derivatives have an electron-withdrawing groups such as $-Cl$ and $-NO_2$ which may decrease the electron density on molecules, but in the case of CMQ, since the electron pair of Cl are shared with phenyl group, it becomes a donor by mesomeric effect and increase the electron density on CMQ, this is why the CMQ compound is better inhibitor than MNQ.

Conclusions

- (1) The quionazolin derivatives inhibit the corrosion of carbon steel in 2 M HCl
- (2) The inhibition is due to adsorption of the inhibitor molecules on the carbon steel surface by blocking its active sites.
- (3) Adsorption of quionazolin derivatives fits Langmuir isotherm.
- (4) Results obtained from weight loss, DC polarization, AC impedance and EFM techniques are reasonably in good agreement and show increased inhibitor efficiency with increasing inhibitor concentration.
- (5) Polarization data showed that the investigated inhibitors act as mixed-type inhibitor in 2 M HCl solution.

REFERENCES

- Abboud Y, Abourriche A, Saffag T, Berrada M, Charrouf M, Bennamara A, Al Himidi N, Hannache H (2007). 2,3-Quinoxalinedione as a novel corrosion inhibitor for mild steel in 1 M HCl Mater. Chem. Phys. 105:1-5.
- Abd El-Maksous SA, Fouda AS (2005). Some pyridine derivatives as corrosion inhibitors for carbon steel in acidic medium, Mater. Chem. Phys. 93(1):84-90.
- Abdallah M, Helal EA, Fouda AS (2006). Aminopyrimidine derivatives as inhibitors for corrosion of 1018 carbon steel in nitric acid solution, Corros. Sci. 48(7):1639-1654.
- Ajmal M, Mideen AS, Quraishi MA (1994). 2-hydrazino-6-methyl-benzothiazole as an effective inhibitor for the corrosion of mild steel in acidic solutions, Corros. Sci. 36(1):79-84.

- Akust AA, Lorenz WJ, Mansfeld F (1982). The determination of corrosion rates by electrochemical d.c. and a.c. methods — II. Systems with discontinuous steady state polarization behavior, *Corros. Sci.* 22(7):611-619.
- Ashassi-sorkhabi H, Magidi MR, Seyyedi K, (2004). Investigation of inhibition effect of some amino acids against steel corrosion in HCl solution, *Appl. Surf. Sci.* 225(1-4):176-185.
- Avci G (2008). Corrosion inhibition of indole-3-acetic acid on mild steel in 0.5 M HCl, *Colloids Surf. A*, 317(1-3):730-736.
- Benali O, Larabi L, Traisnel M, Gengembra L, Harwk Y (2007). Electrochemical, theoretical and XPS studies of 2-mercapto-1-methylimidazole adsorption on carbon steel in 1 M HClO₄, *Appl. Surf. Sci.* 253(14):6130-6139.
- Bentiss F, Lebrini M, Lagrenee M, (2005). Thermodynamic characterization of metal dissolution and inhibitor adsorption processes in mild steel/2,5-bis(*n*-thienyl)-1,3,4-thiadiazoles/hydrochloric acid system, *Corros. Sci.* 47(12):2915-2931.
- Bosch RW, Hubrecht J, Bogaerts WF, Syrett BC (2001). Electrochemical Technique for Online Corrosion Monitoring *Corrosion* 57(1):60-70.
- Deyab MA (2007). Effect of cationic surfactant and inorganic anions on the electrochemical behavior of carbon steel in formation water, *Corros. Sci.* 49(5):2315-2328.
- Donahue FM, Nobe K (1965). Theory of Organic Corrosion Inhibitors: Adsorption and Linear Free Energy Relationships *J. Electrochem. Soc.* 112(9):886-891.
- El Achouri M, Kertit S, Gouttaya HM, Nciri B, Bensouda Y, Perez L, Infante MR, Elkacemi K (2001). Corrosion inhibition of iron in 1 M HCl by some gemini surfactants in the series of alkanediyl- α,ω -bis-(dimethyl tetradecyl ammonium bromide), *Prog. Org. Coat.* 43(4):267-273.
- Fouda AS, Al-Sarawy AA, El-Katori EE (2006a). Potentiometric and thermodynamic studies of 3-methyl-1-phenyl- $\{p$ -[*N*-(pyrimidin-2-yl)-sulfamoyl]phenylazo}-2-pyrazolin-5-one and its metal complexes, *Chem. Paper* 60(1):5-9.
- Fouda AS, Al-Sarawy AA, El-Katori EE (2006b). Pyrazolone derivatives as corrosion inhibitors for C-steel HCl solution," *Desalination*, 201:1-13.
- Gao X, Cai X, Yan K, Song B, Gao L (2007). Synthesis and characterization of some organic compounds, *Z.Chem., Mol.* 12(12):2621-2642.
- Growcock FB, Jasinski JH (1989). Time-Resolved Impedance Spectroscopy of Mild Steel in Concentrated Hydrochloric Acid, *J. Electrochem. Soc.* 136(8):2310-2314.
- Hammett LP (1940). *Physical Organic Chemistry*" McGraw-Hill Book Co., N.Y.
- Hsu CH, Mansfeld F (2001). Concerning the conversion of the constant phase element parameter Y0 into a capacitance, *Corros.* 57(9):747-748.
- Ishtiaque A, Rajendra P, Quraishi MA (2010). Inhibition of mild steel corrosion in acid solution by Pheniramine drug: Experimental and theoretical study, *Corros. Sci.* 52(9):3033-3041.
- Jovancevic V, Yang B, O'M.Bockris J (1988). Adsorption, Orientation, and Polymerization of 1-Octyne-3-ol on Iron: An Ellipsometric Study, *J. Electrochem. Soc.* 135(1):94-98.
- Kelly RG, Scully JR, Shoesmith DW, Buchheit RG (2002). *Electrochemical Techniques in Corrosion Science and Engineering*, Marcel Dekker, Inc., New York, P. 148.
- Khaled KF (2003). The inhibition of benzimidazole derivatives on corrosion of iron in 1 M HCl solutions, *Electrochim. Acta.* 48:2493-2503.
- Khaled KF (2008). Guanidine derivative as a new corrosion inhibitor for copper in 3% NaCl solution, *Mater. Chem. Phys.* 122:290-300.
- Khamis E, Bellucci F, Latanision RM, El-Ashry ESH (1991). Acid corrosion inhibition of nickel by 2-(Triphenosporanylidene) succinic anhydride, *Corros.* 47(9):677-686.
- Lebrini M, Lagrenee M, Traisnel M, Gengembra L, Vezin H, Bentiss F (2007). Enhanced corrosion resistance of mild steel in normal sulfuric acid medium by 2,5-bis(*n*-thienyl)-1,3,4-thiadiazoles: Electrochemical, X-ray photoelectron spectroscopy and theoretical studies, *Appl. Surf. Sci.* 253(23):9267-9276.
- Machnikova E, Pazderova M, Bazzouai M, Hackerman N (2008a). Corrosion study of PVD coatings and conductive polymer deposited on mild steel: Part I: Polypyrrole, *Surf. Coat. Technol.* 202(8):1543-1550
- Machnikova E, Whitmire KH, Hackerman N (2008b). Corrosion inhibition of carbon steel in hydrochloric acid by furan derivatives, *Electrochim. Acta*, 53:6024-6032.
- Mehaute AH, Grepy G (1983). Introduction to transfer and motion in fractal media: The geometry of kinetics, *Solid State Ionics*, 9(10):17-30.
- Migahed MA, Nasser IF (2008). Corrosion inhibition of Tubing steel during acidization of oil and gas wells, *Electrochim. Acta.* 53:2877-2882.
- Noot EA, Al-Moubaraki AH (2008). Thermodynamic study of metal corrosion and inhibitor adsorption processes in mild steel/1-methyl-4[4'(-X)-styryl pyridinium iodides/hydrochloric acid systems, *Mater. Chem. Phys.* 110:145-154.
- O'M Bockris J, Yang B (1991). The Mechanism of Corrosion Inhibition of Iron in Acid Solution by Acetylenic Alcohols, *J. Electrochem. Soc.* 138(8):2237-2252.
- Pillali KC, Narayan R (1985). Anodic dissolution of mild steel in HCl solutions containing thio-ureas, *Corros.Sci.* 23(2):151-166.
- Popova A, Chistov M, Raicheva S, Sokolova E (2004). Adsorption and inhibitive properties of benzimidazole derivatives in acid mild steel corrosion, *Corros. Sci.* 46(6):1333-1350.
- Rammet U, Reinhart G (1987). The influence of surface roughness on the impedance data for iron electrodes in acid solutions, *Corros. Sci.* 27(4):373-382.
- Singh AK, Quraishi MA (2010). Inhibitive effect of diethylcarbamazine on the corrosion of mild steel in hydrochloric acid, *Corros. Sci.* 52(4):1529-1535.
- Uhera J, Aramaki K (1991). Surface-Enhanced Raman Spectroscopy Study on Adsorption of Some Sulfur-Containing Corrosion Inhibitors on Iron in Hydrochloric Acid Solutions *J. Electrochem. Soc.* 138(11):3245-3251.
- Zhao TP, Mu GN (1999). The adsorption and corrosion inhibition of anion surfactants on aluminium surface in hydrochloric acid, *Corros. Sci.* 41(10):937-944.